

# Sagnac Effect of Gödel's Universe

E. Kajari\*, R. Walser and W. P. Schleich

Abteilung für Quantenphysik, Universität Ulm, 89069 Ulm, Germany

A. Delgado

Departamento de Física, Universidad de Concepción,  
Casilla 160-C, Concepción, Chile

23rd October 2018

## Abstract

We present exact expressions for the Sagnac effect of Gödel's Universe. For this purpose we first derive a formula for the Sagnac time delay along a circular path in the presence of an arbitrary stationary metric in cylindrical coordinates. We then apply this result to Gödel's metric for two different experimental situations: First, the light source and the detector are at rest relative to the matter generating the gravitational field. In this case we find an expression that is formally equivalent to the familiar nonrelativistic Sagnac time delay. Second, the light source and the detector are rotating relative to the matter. Here we show that for a special rotation rate of the detector the Sagnac time delay vanishes. Finally we propose a formulation of the Sagnac time delay in terms of invariant physical quantities. We show that this result is very close to the analogous formula of the Sagnac time delay of a rotating coordinate system in Minkowski spacetime.

---

\*email: endre.kajari@physik.uni-ulm.de

# 1 Introduction

Phenomena in rotating coordinate systems have fascinated scientists since hundreds of years. Three examples may serve as an illustration of this statement: *i)* The Coriolis force is instrumental in the demonstration of the rotation of the earth with the help of the Foucault pendulum [1]. *ii)* The Sagnac effect [2, 3, 4, 5, 6] measured by the Michelson-Gale-interferometer [7] is the analogous optical tool. *iii)* Mach's principle [8, 9, 10] ushers in a fresh view on the relativity of rotation. In the present paper we combine these three concepts and calculate the Sagnac effect of Gödel's Universe.

Einstein's theory of General Relativity [11] predicts gravito-magnetic forces [12, 13, 14] due to the rotation of massive objects. These forces give rise to the precession of nodal lines [15] of two orbiting LAGEOS-satellites proving the first measurement of the Lense-Thirring effect [16, 17, 18, 19]. The newly emerging field of atom optics has opened a new arena [20] for measuring the dipole character of the Lense-Thirring field with the help of an atom gyroscope [21, 22, 23, 24].

Rotation is not limited to a coordinate system or individual masses but even the universe can display features of rotation. Indeed, in 1949 Kurt Gödel [25, 26, 27] derived an exact solution of Einstein's field equations, in which a homogeneous mass distribution rotates around every point in space. This solution shows rather unusual properties [28] such as closed time like world-lines.

In a recent paper [29] we have evaluated the Sagnac effect of Gödel's Universe measured in a laboratory size interferometer. For this purpose we have used the linearized Gödel metric, which can be approximated by the flat spacetime metric of a rotating coordinate system. In the present paper we calculate the exact Sagnac effect for the Gödel metric.

## 1.1 Why Gödel's Metric?

Gödel's Universe has many fascinating features. Indeed, the inherent rotation of this Universe is only one interesting aspect. Even more intriguing is the lack of a global time ordering and the existence of closed time like world lines giving rise to the possibility of time travel. Such causal problems emerge also in other exact solutions of Einstein's field equations, such as the Kerr metric. However, Gödel's metric has the advantage that it is of rather compact form and most calculations can be carried out analytically.

It is commonly accepted that this model does not provide a matching description of our observed universe. Nevertheless, there is the emerging field of experimental cosmology in the laboratory [30]. In particular, the examination of wave phenomena in curved spacetimes is a focus of research. For example, optical analogues of black holes have been proposed by studying light propagation in moving media [31] or sound propagation in condensed matter systems [32, 33]. In this context, it is important to ask how far one can extend such analogues in general. Gödel's Universe can shed some light on this problem, since the existence of closed time like world lines curtails the expectation of a globally valid experimental analogue. Thus, it would be interesting to see, where and how the experimental realization ceases to exist.

Motivated by this idea we have initiated a study of wave propagation for the source free Maxwell equations in Gödel's metric [34, 35]. However, in the present paper we will focus on the Sagnac time delay within the limit of geometrical optics and draw the comparison to the Sagnac time delay in a rotating frame in flat Minkowski spacetime [29]. In order to keep the paper self-contained and in view of the fact that this issue brings together researches from atomic, molecular and optical physics with experts in General Relativity we have used this opportunity to combine our study of the Sagnac effect with a mini review of Gödel's Universe.

## 1.2 Outline of the Paper

Our paper is organized as follows: In Section 2 we first briefly review the essential features of the Sagnac effect and then derive an exact expression for the Sagnac time delay for a time independent metric in cylindrical coordinates. We dedicate Section 3 to a discussion of the Gödel metric. We then apply in Section 4 the expression of the Sagnac time delay to Gödel's metric. In Section 5 we reformulate the Sagnac effect purely in terms of proper time delays of light pulses and compare it to the analogous expression for a rotating frame in flat Minkowski spacetime. We conclude by an outlook to possible laboratory realizations of the local light propagation in Gödel's Universe.

## 2 Sagnac Effect: Basics

In the present section we first recall the familiar Sagnac effect and then derive an exact expression for the Sagnac time delay in terms of metric coefficients. We conclude by making contact with the familiar Sagnac effect using the metric of a rotating coordinate system in flat Minkowski spacetime.

### 2.1 Familiar Sagnac Time Delay

In 1913 George Sagnac performed an experiment [2, 3], which he interpreted as an verification of the existence of the ether. In order to bring out the essential features of this phenomenon we consider two counter-propagating light pulses which travel on a circle of radius  $r_0$  due to an appropriate array of mirrors or a glass fiber. When the setup is at rest the two counter-propagating pulses arrive at the same time at the point of emission. However, when the arrangement rotates there is a time delay between them. This Sagnac time delay  $\Delta t_S$  follows from an elementary, classical argument [36] and reads

$$\Delta t_S \approx \frac{4\Omega_R}{c^2} \pi r_0^2. \quad (1)$$

Hence,  $\Delta t_S$  is proportional to the area  $\pi r_0^2$  enclosed by the light beams and the rotation rate  $\Omega_R$  of the ring with respect to the flat Minkowski spacetime. Moreover, we note that this result is an approximation and higher order corrections in  $\Omega_R$  will arise as discussed in Section 2.3.

The Sagnac effect is the basis of modern navigational systems. Moreover, it can also be generalized in the framework of General Relativity [12, 37], as presented in the next section. In particular, the Sagnac effect is closely related to the Hannay angle [38] and the synchronization of clocks [39] along a closed path.

## 2.2 Time Delay for a Stationary Metric

We now derive an exact expression for the Sagnac time delay  $\Delta\tau_S$  in terms of the time independent metric coefficients  $g_{\mu\nu}$  expressed in cylindrical coordinates  $x^\mu \equiv (x^0, x^1, x^2, x^3) \equiv (t, r, \phi, z)$ . For a general treatment of the Sagnac effect of two counterpropagating light rays along any spatially closed path in an arbitrary metric we refer to [40]. However, inhere we choose a particularly simple configuration and consider the propagation along a circle of radius  $r_0$  in the  $z = z_0$  plane resulting in  $dx^1 = dr = 0$  and  $dx^3 = dz = 0$ . For this situation the line element reads

$$ds^2 = g_{\mu\nu} dx^\mu dx^\nu = g_{00}(dx^0)^2 + 2g_{02} dx^0 dx^2 + g_{22}(dx^2)^2, \quad (2)$$

and vanishes for light  $ds^2 = 0$ .

The angular velocity

$$\omega \equiv \frac{dx^2}{dx^0} \quad (3)$$

of the light beam follows from the quadratic equation

$$g_{22} \omega^2 + 2g_{02} \omega + g_{00} = 0,$$

giving rise to the two velocities

$$\omega_{\pm} = -\frac{g_{02}}{g_{22}} \pm \sqrt{\left(\frac{g_{02}}{g_{22}}\right)^2 - \frac{g_{00}}{g_{22}}}. \quad (4)$$

In order to get two solutions, which correspond to two ordinary counter-propagating light beams, we restrict ourselves to spacetime regions  $G$ , in which the above metric coefficients satisfy the conditions

$$g_{00} > 0, \quad g_{22} < 0 \quad \forall x^\mu \in G. \quad (5)$$

These conditions immediately imply that the angular velocity  $\omega_+$  is positive and  $\omega_-$  is negative for all events in  $G$ , so that the monotony of the corresponding solutions  $x_{\pm}^0(x^2)$  is guaranteed. The condition  $g_{00} > 0$  is furthermore important to allow for an observer resting relative to the chosen spatial coordinates and measuring the proper time, as discussed e.g. in [41].

We can find the coordinate times  $x_{\pm}^0$  of the first return of the counter-propagating light rays to their starting point  $x^2 = \phi_0$  by integrating equation (3) over one period  $2\pi$  in positive and negative angular direction, respectively. Hence, we arrive at

$$x_{\pm}^0 = \int_{\phi_0}^{\phi_0 \pm 2\pi} \frac{dx^2}{\omega_{\pm}} = \pm \int_0^{2\pi} \frac{dx^2}{\omega_{\pm}}, \quad (6)$$

where in the second step we have made use of the periodicity of the metric coefficients in the coordinate  $x^2$ .

When we recall the connection  $d\tau = \sqrt{g_{00}(r_0, \phi_0, z_0)} dx^0/c$  between the coordinate time  $x^0$  and the proper time  $\tau$  measured by an observer resting at  $(r_0, \phi_0, z_0)$ , the corresponding proper times  $\tau_{\pm}$  of the incoming light rays read

$$\tau_{\pm} = \pm \frac{1}{c} \sqrt{g_{00}(r_0, \phi_0, z_0)} \int_0^{2\pi} \frac{dx^2}{\omega_{\pm}}. \quad (7)$$

The positive sign in  $\tau_+$  corresponds to the light pulse propagating in the positive angular direction, whereas the negative sign in  $\tau_-$  denotes the proper time of the light pulse traveling in the negative angular direction.

The Sagnac proper time delay  $\Delta\tau_S$  follows as

$$\Delta\tau_S \equiv (\tau_+ - \tau_-) = \frac{1}{c} \sqrt{g_{00}(r_0, \phi_0, z_0)} \int_0^{2\pi} \frac{\omega_+ + \omega_-}{\omega_+ \omega_-} dx^2,$$

which reduces with help of the explicit expressions (4) for  $\omega_{\pm}$  to

$$\Delta\tau_S = -\frac{2}{c} \sqrt{g_{00}(r_0, \phi_0, z_0)} \int_0^{2\pi} \frac{g_{02}}{g_{00}} dx^2. \quad (8)$$

If we further assume, that the metric coefficients  $g_{02}$  and  $g_{00}$  do not depend on the angular coordinate  $x^2$ , then the expression (8) for the Sagnac time delay reduces to the compact formula

$$\Delta\tau_S = -\frac{4\pi}{c} \frac{g_{02}}{\sqrt{g_{00}}}. \quad (9)$$

For negative values of  $\Delta\tau_S$  the light pulse which propagates in the positive angular direction returns before the other pulse and vice versa for positive  $\Delta\tau_S$ .

We conclude by noting that the Sagnac time delay (9) is by construction only form-invariant under the special class of coordinate transformations

$$x'^0 = x^0(x^0, x^1, x^3), \quad x'^1 = x^1(x^1, x^3), \quad x'^2 = x^2, \quad x'^3 = x^3(x^1, x^3),$$

which change neither the frame of reference nor the angular coordinate.

### 2.3 Time Delay in a Rotating Frame

We now want to apply formula (9) of the Sagnac time delay to the metric of a rotating coordinate frame in flat Minkowski spacetime. The line element in flat Minkowski spacetime reads in cylindrical coordinates  $x^\mu = (t, r, \phi, z)$

$$ds^2 = c^2 dt^2 - dr^2 - r^2 d\phi^2 - dz^2. \quad (10)$$

The coordinates  $x'^{\mu} = (t', r', \phi', z')$  of a reference frame rotating with a rate  $\Omega_R > 0$  are defined by the transformation equations

$$t \equiv t', \quad r \equiv r', \quad \phi \equiv \phi' + \Omega_R t', \quad z \equiv z',$$

and give rise to a line element  $ds^2 = g'_{\mu\nu} dx'^{\mu} dx'^{\nu}$  of the form

$$ds^2 = (c^2 - r'^2 \Omega_R^2) dt'^2 - dr'^2 - r'^2 d\phi'^2 - dz'^2 - 2r'^2 \Omega_R dt' d\phi'. \quad (11)$$

To satisfy the conditions (5) we have to restrict ourselves to the spacetime region

$$G' \equiv \left\{ 0 \leq r' < \frac{c}{\Omega_R}, 0 \leq \phi' < 2\pi, -\infty < t', z' < \infty \right\}. \quad (12)$$

When we now assume that the counter-propagating light rays travel along a circle with radius  $r'_0$  and substitute the metric coefficients  $g'_{00}$  and  $g'_{02}$  into (9), the Sagnac time delay in the rotating frame reads

$$\Delta\tau'_R = \frac{4\pi}{c^2} \frac{r'^2_0 \Omega_R}{\sqrt{1 - \left(\frac{r'_0 \Omega_R}{c}\right)^2}}. \quad (13)$$

In the first approximation of  $(r'_0 \Omega_R / c)$  this expression reduces to the time delay of the familiar Sagnac effect (1).

However, also the limit of large rotation rates, where the square root in the denominator gets important is of interest. Indeed, in Section 5 we present an expression for the Sagnac time delay in Gödel's Universe, which on first sight looks very different from (13). Nevertheless, a closer view reveals that this formula is numerically very close to the Minkowskian Sagnac time delay.

### 3 Essential Features of Gödel's Universe

In order to gain some insight into the intricacies of Gödel's Universe we briefly review two representations of Gödel's metric that are convenient for our analysis of the Sagnac effect. Moreover, we sketch the conditions under which this metric solves Einstein's field equations. We then present tensorial quantities characterizing the time like velocity field of the matter generating the Gödel metric. Furthermore, we make contact with the metric of flat spacetime in cylindrical coordinates and mention the symmetries and the causal structure of Gödel's metric. We conclude this section by summarizing special null geodesics, which will be important in expressing the Sagnac time delay by measurable quantities.

#### 3.1 Line Element and Einstein's Field Equations

The line element  $ds^2 \equiv \bar{g}_{\mu\nu} d\bar{x}^{\mu} d\bar{x}^{\nu}$  given by Gödel [25] in 1949 in dimensionless, cylindrical coordinates  $\bar{x}^{\mu} \equiv (\bar{x}^0, \bar{x}^1, \bar{x}^2, \bar{x}^3) \equiv (\bar{t}, \bar{r}, \bar{\phi}, \bar{z})$  with

$$G_G \equiv \left\{ -\infty < \bar{t} < \infty, 0 \leq \bar{r} < \infty, 0 \leq \bar{\phi} < 2\pi, -\infty < \bar{z} < \infty \right\}, \quad (14)$$

has the form

$$\frac{ds^2}{4a^2} = d\bar{t}^2 - d\bar{r}^2 - (\sinh^2 \bar{r} - \sinh^4 \bar{r}) d\bar{\phi}^2 - d\bar{z}^2 + 2\sqrt{2} \sinh^2 \bar{r} d\bar{\phi} d\bar{t}. \quad (15)$$

The parameter  $a > 0$  has the unit of a length.

In the next section we derive a simple expression for the Sagnac effect. For this purpose, it is convenient to use a slightly different form of Gödel's metric, which can be obtained from (15) by the coordinate transformation

$$t \equiv \frac{2a}{c} \bar{t}, \quad r \equiv 2a \sinh \bar{r}, \quad \phi \equiv \bar{\phi}, \quad z \equiv 2a \bar{z}. \quad (16)$$

The resulting line element reads

$$ds^2 = c^2 dt^2 - \frac{dr^2}{1 + \left(\frac{r}{2a}\right)^2} - r^2 \left(1 - \left(\frac{r}{2a}\right)^2\right) d\phi^2 - dz^2 + 2r^2 \frac{c}{\sqrt{2a}} dt d\phi. \quad (17)$$

These new coordinates have now physical dimensions.

We can convince ourselves that the metric coefficients

$$(g_{\mu\nu}) = \begin{pmatrix} c^2 & 0 & r^2 \frac{c}{\sqrt{2a}} & 0 \\ 0 & -\frac{1}{1 + \left(\frac{r}{2a}\right)^2} & 0 & 0 \\ r^2 \frac{c}{\sqrt{2a}} & 0 & -r^2 \left(1 - \left(\frac{r}{2a}\right)^2\right) & 0 \\ 0 & 0 & 0 & -1 \end{pmatrix} \quad (18)$$

corresponding to the line element (17) indeed solve Einstein's field equations

$$R_{\mu\nu} - \frac{1}{2} g_{\mu\nu} R = \kappa T_{\mu\nu} + \Lambda g_{\mu\nu},$$

by calculating explicitly the Ricci tensor  $R_{\mu\nu}$  and the scalar curvature  $R$ , defined in Appendix A. Here  $\Lambda$  denotes the cosmological constant and  $\kappa \equiv (8\pi G)/(c^4)$  with Newton's gravitational constant  $G$  and the velocity of light  $c$ .

The energy momentum tensor  $T_{\mu\nu}$  of an ideal fluid with mass density  $\rho$  and pressure  $p$  reads

$$T_{\mu\nu} \equiv \left(\rho + \frac{p}{c^2}\right) u_\mu u_\nu - p g_{\mu\nu}.$$

With the four-velocity  $u^\mu = (1, 0, 0, 0)$  of the matter generating the field, we find

$$R_{\mu\nu} = \frac{u_\mu u_\nu}{a^2 c^2}, \quad R = \frac{1}{a^2}.$$

When we substitute these expressions into the field equations, we arrive at the two relations

$$\kappa \left(\rho + \frac{p}{c^2}\right) = \frac{1}{a^2 c^2}, \quad \kappa p = \Lambda + \frac{1}{2a^2},$$

which couple the length scale  $a$  to the density  $\rho$ , the pressure  $p$  and the cosmological constant  $\Lambda$ .

### 3.2 Time Like Velocity Field of the Ideal Fluid

The essential properties of the motion of the ideal fluid generating the field are characterized by the tensorial quantities  $\theta$ ,  $\sigma_{\alpha\beta}$  and  $\omega_{\alpha\beta}$  representing the volume expansion, the shear tensor and the rotation tensor, respectively [28, 42]. From the four-velocity  $u^\mu \equiv (1, 0, 0, 0)$  and the acceleration  $a^\mu = u^\mu_{;\nu} u^\nu = 0$  of the congruence of time like curves belonging to the ideal fluid we find a vanishing volume expansion

$$\theta \equiv u^\mu_{;\mu} = 0,$$

and a vanishing shear tensor

$$\sigma_{\alpha\beta} \equiv P^\mu_\alpha P^\nu_\beta u_{(\mu;\nu)} - \frac{1}{3}\theta P_{\alpha\beta} = 0.$$

Here we have introduced the projection tensor

$$P^\alpha_\beta \equiv \delta^\alpha_\beta - \frac{1}{c^2} u^\alpha u_\beta$$

together with  $u_{(\mu;\nu)} \equiv (u_{\mu;\nu} + u_{\nu;\mu})/2$ , where the semicolon denotes the covariant derivative.

However, we arrive at a non-vanishing rotation tensor

$$\omega_{\alpha\beta} \equiv P^\mu_\alpha P^\nu_\beta u_{[\mu;\nu]} = u_{[\alpha;\beta]} = r \frac{c}{\sqrt{2a}} (\delta^2_\alpha \delta^1_\beta - \delta^2_\beta \delta^1_\alpha). \quad (19)$$

Here the square brackets are defined by  $u_{[\mu;\nu]} \equiv (u_{\mu;\nu} - u_{\nu;\mu})/2$  and the comma denotes the partial derivative.

The corresponding rotation vector

$$\omega^\alpha \equiv \frac{1}{2} \varepsilon^{\alpha\beta\gamma\delta} u_\beta u_{\gamma;\delta} = \frac{c^2}{\sqrt{2a}} \delta^3_\alpha \quad (20)$$

and the rotation scalar

$$\Omega_G \equiv \sqrt{\frac{1}{2} \omega^{\alpha\beta} \omega_{\alpha\beta}} = \frac{c}{\sqrt{2a}} > 0. \quad (21)$$

are constant in every point of Gödel's Universe.

In the limit  $a \rightarrow \infty$  all rotation quantities (19), (20) and (21) vanish. Moreover, for  $r/(2a) \ll 1$  we find that the line element (17) can be approximated in first order by

$$ds^2 = c^2 dt^2 - dr^2 - r^2 d\phi^2 - dz^2 + 2r^2 \Omega_G dt d\phi + \mathcal{O}(\Omega_G^2).$$

While the zeroth order approximation [43] corresponds to the line element (10) of flat spacetime in cylindrical coordinates the linear correction is reminiscent of the line element (11) of a rotating coordinate frame in Minkowski spacetime.



### 3.3 Killing Vectors and Symmetry

If a spacetime manifold with the metric  $g_{\mu\nu}$  possesses symmetries, then they can be characterized by a special class of coordinate transformations  $x'^\alpha = x'^\alpha(x^\beta)$  which satisfy the condition

$$g'_{\mu\nu}(x'^\alpha) = g_{\mu\nu}(x^\alpha). \quad (22)$$

Such a coordinate transformation is called isometry. In particular, the infinitesimal isometries

$$x'^\alpha = x^\alpha + \varepsilon \xi^\alpha(x^\beta) \quad (23)$$

with  $\varepsilon \ll 1$  are of special interest, since every continuous isometry can be constructed successively by these infinitesimal isometries.

The infinitesimal transformation (23) together with (22) and the transformation law of a metric yields the condition

$$\xi_{\alpha;\beta} + \xi_{\beta;\alpha} = 0 \quad (24)$$

for the Killing vector field  $\xi^\alpha(x^\beta)$ . The solutions  $\xi^\alpha$  of this linear system of partial differential equations characterize the symmetry of a given metric.

In the case of Gödel's metric we find five Killing vectors as solutions of the Killing equation (24). Three of them are immediately found from (22), since Gödel's metric does not depend explicitly on the coordinates  $(t, \phi, z)$ . With the constants  $A, B, C, D, E$  the complete solution of (24) reads

$$\xi^\alpha(t, r, \phi, z) = A\delta_0^\alpha + B\delta_2^\alpha + C\delta_3^\alpha + D\zeta^\alpha(r, \phi) + E\zeta^\alpha(r, \phi - \frac{\pi}{2}), \quad (25)$$

with

$$\begin{pmatrix} \zeta^0 \\ \zeta^1 \\ \zeta^2 \\ \zeta^3 \end{pmatrix} \equiv \frac{1}{\sqrt{1 + \left(\frac{r}{2a}\right)^2}} \begin{pmatrix} \frac{r}{\sqrt{2c}} \cos \phi \\ a \left(1 + \left(\frac{r}{2a}\right)^2\right) \sin \phi \\ \frac{a}{r} \left(1 + 2 \left(\frac{r}{2a}\right)^2\right) \cos \phi \\ 0 \end{pmatrix}.$$

Since (25) contains a time like Killing vector Gödel's Universe is stationary. Moreover it is also spatially homogeneous. However, a more detailed analysis of the Killing vectors shows, that Gödel's metric is not static and also not isotropic. The latter feature is due to the existence of a rotational axis giving rise to a rotational symmetry in the  $z = \text{const.}$  planes.

### 3.4 Causal Structure

The non-vanishing rotation scalar has a dramatic consequence for the causal structure of Gödel's Universe. In order to gain some insight into this feature, it is useful to consider infinitesimal light cones at different spatial points. Figure 1 depicts such an arrangement. The cylindrical coordinates  $(t, r, \phi, z)$  are embedded for illustration in a Cartesian frame

$$(t, x \equiv r \cos \phi, y \equiv r \sin \phi, z) \quad (26)$$

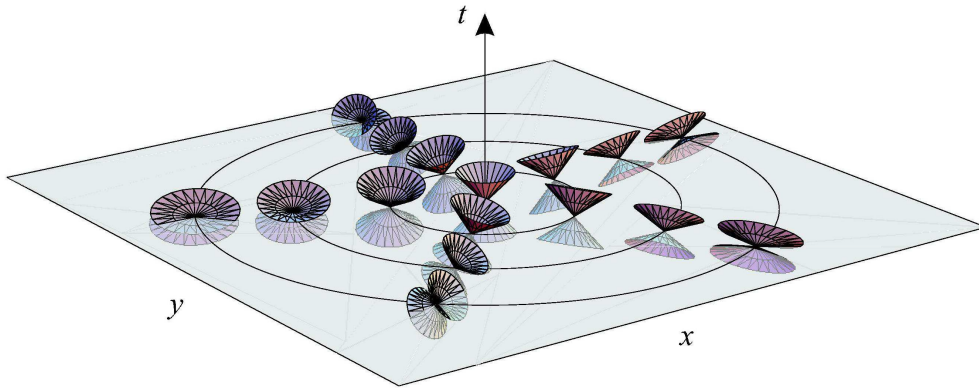


Figure 1: Light cones in Gödel's metric represented in the  $z = 0$  plane. The middle circle of critical radius  $r_G = 2a$  separates the domains of different causal behavior. At every point of the inner domain the light cones lie outside of the  $t = 0$  plane as exemplified by the cones along the inner circle. In contrast, outside of the critical circle the cones cut through this plane.

and the third spatial coordinate  $z$  is suppressed in the figure. For every instant of time there exists a domain in space with closed time like world-lines. To visualize this property, we consider the orientation of some selected light cones with respect to the plane of constant coordinate time  $t$ .

At the origin of the coordinate system the axis of the light cone is orthogonal to the plane. As we move away from the origin the light cones start to tilt, as indicated in Figure 1. At the critical Gödel radius  $r_G = 2a$ , represented by the middle circle, the light cones are tangential to the plane of constant coordinate time  $t$ . This circle of radius  $r_G$  is a light like curve. Outside this critical radius the inclination of the light cones increases further and allows the existence of closed time like curves, as shown by the outer circle in Figure 1.

It is this peculiar feature of the causal structure which permits to connect two arbitrary events of spacetime by a time like curve, irrespectively of their ordering in the chosen coordinate time  $t$ . Indeed, we can start from a point within the inner circle and cross the critical Gödel radius to explore the world beyond this border. During this trespassing we take a time like world line which spirals downwards into the past. Having regressed long enough on this trajectory we can finally return to the original causal domain, thus arriving before departing.

We conclude by noting that closed time like world-lines are not limited to Gödel's Universe. They also appear in other exact solutions of Einstein's field equations for rotating mass distributions. Examples include the rotating Kerr black hole [44, 45] and the van Stockum rotating dust cylinder [46]. Most recently it has been shown [47], that the gravitational field of a solenoid of light, that is a light beam bent along helical path also exhibits such closed time like world-lines.

### 3.5 Null Geodesics

In the presence of a metric, the free motion of particles or the propagation of light rays is described by the geodesic equations

$$\frac{d^2 x^\mu}{d\lambda^2} + \Gamma^\mu_{\alpha\beta} \frac{dx^\alpha}{d\lambda} \frac{dx^\beta}{d\lambda} \equiv u^\mu{}_{;\nu} u^\nu = 0 \quad (27)$$

and by the condition

$$g_{\mu\nu} u^\mu u^\nu = \epsilon^2.$$

For the definition of the Christoffel symbols  $\Gamma^\mu_{\alpha\beta}$  we refer to Appendix A and  $x^\mu(\lambda) = (t(\lambda), r(\lambda), \phi(\lambda), z(\lambda))$  is the path of the particle or light beam. For massive particles  $\epsilon$  denotes the velocity  $c$  of light and the curve parameter  $\lambda$  represents its proper time. Moreover, the tangent vector  $u^\mu \equiv dx^\mu/d\lambda$  is the four-velocity of the particle. In the case of a light beam we have to set  $\epsilon = 0$  and the curve parameter  $\lambda$  has no physical meaning. The solutions of the geodesic equations for Gödel's metric were first given by W. Kundt [48], independently examined by S. Chandrasekhar and J.P. Wright [49] and discussed in detail by Novello et. al. [50].

In Section 5 we express the Sagnac time delay in measurable quantities only. For this purpose we need to know the geodesic motion of light for special initial conditions. Indeed, the light pulse shall start for the initial curve parameter  $\lambda_0 = 0$  at the point  $r(0) = 0$ ,  $z(0) = 0$ . Furthermore, the light ray shall have a vanishing  $z$ -component of the initial velocity, that is  $u^3(0) = 0$ . Since we start at the origin, the radial velocity has to be positive, that is  $u^1(0) > 0$ .

In Appendix B we outline a procedure for obtaining the general solution of the geodesic equations (27) for Gödel's metric and integrate these equations subjected to these initial conditions.

For the radial coordinate we find the expression

$$\frac{r(\lambda)}{2a} = \left| \sin \left( \frac{1}{2} \eta \lambda \right) \right|, \quad (28)$$

where we have introduced the abbreviation

$$\eta \equiv \sqrt{2} u^0(0) \Omega_G. \quad (29)$$

Hence, when the curve parameter  $\lambda$  reaches the value  $\lambda_c \equiv (2\pi)/\eta$  the light pulse returns again to the origin  $r = 0$ .

The coordinate time along these geodesics reads

$$t(\lambda) = -u^0(0) \lambda + \frac{2}{\Omega_G} \left[ \arctan \left( \sqrt{2} \tan(\eta\lambda/2) \right) + m(\lambda) \pi \right], \quad (30)$$

where the integer

$$m(\lambda) \equiv \left[ \frac{\eta\lambda}{2\pi} + \frac{1}{2} \right]_I \quad (31)$$

represents the greatest integer less than or equal to the number inside the brackets.

Within one cycle,  $0 \leq \lambda \leq 2\pi/\eta$ , the coordinate time  $t(\lambda)$  increases by the time interval

$$\Delta t_c = \frac{\sqrt{2}\pi}{\Omega_G} (\sqrt{2} - 1).$$

For the angle coordinate  $\phi(\lambda)$  the integration yields

$$\phi(\lambda) = \phi(0) + \arctan\left(\sqrt{2}\tan(\eta\lambda/2)\right) + [m(\lambda) - m(\lambda - \pi/\eta)]\pi. \quad (32)$$

We conclude this section by illustrating the null geodesics for the special initial conditions in Figure 2. The left side displays the geodesic motion in the  $(x, y)$ -plane embedded in

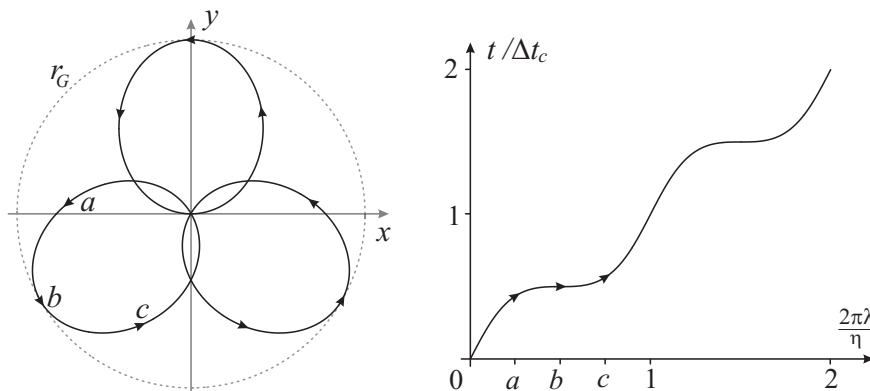


Figure 2: Null geodesics in the  $(x, y)$ -plane (left) and coordinate time  $t(\lambda)$  extending over 2 cycles (right) for the special initial conditions  $r(0) = 0$ ,  $u^3(0) = 0$  and  $\phi(0) = (0, 2\pi/3, 4\pi/3)$ . The three values  $a, b, c$  of the curve parameter  $\lambda$  mark the three different positions on a null geodesic on the left.

the coordinate frame (26). The light signals emitted at the origin  $r = 0$  cycle in the positive angular direction. The right side of the figure shows the coordinate time  $t(\lambda)$  for the increasing curve parameter  $\lambda$ . The inflection points in the time coordinate appear when the light ray touches the critical Gödel radius.

## 4 Sagnac Time Delay in Gödel's Universe

The goal of the present section is to derive an exact expression for the Sagnac time delay of two counter-propagating light rays on a circle in the presence of Gödel's metric. We also analyze the Sagnac effect observed by a detector rotating relative to the ideal fluid. Finally we briefly discuss the dependence of the Sagnac time delay on the choice of the spatial coordinates.

### 4.1 Sagnac Effect in the Rest Frame of the Ideal Fluid

We start by considering a situation in which the emitter and the detector are at rest in the coordinate frame of the ideal fluid. The light pulses propagate along a circle of radius

$r = r_0$  in the plane  $z = z_0$ . Recalling Gödel's metric (18) and the rotation scalar (21) the relevant metric coefficients read

$$g_{00} = c^2, \quad g_{02} = r_0^2 \Omega_G. \quad (33)$$

In order to satisfy the conditions (5), we have to restrict ourselves to the spacetime region

$$G \equiv \{0 \leq r < 2a, 0 \leq \phi < 2\pi, -\infty < t, z < \infty\}.$$

If we do not confine ourselves to this domain the coordinate time needed by one of the light pulses to return to the starting point will be negative for radii larger than the critical Gödel radius  $r_G = 2a$ . This feature follows from the orientation of the future light cones in Figure 1.

Furthermore an observer resting with the detector at  $r_0 > r_G$  would measure a negative proper time of the returning light ray, which travels backward in the coordinate time. By restricting our experimental setup to the region  $G$  we avoid such alien situations in which the light pulse returns before it is emitted with respect to the chosen coordinate time.

When we substitute the coefficients (33) into formula (9) the Sagnac time delay for Gödel's metric reads

$$\Delta\tau_S = -\frac{4\Omega_G}{c^2} \pi r_0^2. \quad (34)$$

Since this expression is negative, we conclude from the definition of the proper time  $\Delta\tau_S$ , that the light pulse propagating in the positive angular direction will always return to its starting point before the pulse propagating in the negative direction.

It is instructive to compare this result to the familiar Sagnac time delay  $\Delta t_S$  given by (1). On first sight the absolute value of the Sagnac time delay (34) in Gödel's Universe seems to be identical to the familiar Sagnac effect (1). However, when we recall that the coordinate  $r_0$  in Gödel's Universe does not represent a proper distance, we recognize that the similarity only arises from the special choice of our spatial coordinates. We will return to this point in Section 4.3.

We conclude by noting that the gravitational time delay in Gödel's Universe has also been calculated in [51]. However, the expression given in that paper is quadratic in the rotation scalar.

## 4.2 Sagnac Effect Measured by a Rotating Detector

We now analyze the Sagnac time delay for a slightly different experimental situation. The light source emitting the two counter-propagating light rays and the detector are now no longer at rest relative to the ideal fluid, but rotate relative to it. We denote the corresponding rotation rate by  $\Omega_D$ . Due to this additional rotation the Sagnac time delay will also depend on  $\Omega_D$ . After providing an explicit expression for the Sagnac time delay for this situation we choose  $\Omega_D$  such, that this time delay vanishes exactly.

We start from the metric (18) and perform the coordinate transformation

$$t \equiv t', \quad r \equiv r', \quad \phi \equiv \phi' + \Omega_D t', \quad z \equiv z'$$

into the rotating frame of the detector. In the new coordinates the line element takes the form

$$ds^2 = \left( c^2 - r'^2 \Omega_D^2 \left( 1 - \frac{r'^2}{4a^2} \right) + 2r'^2 \Omega_D \Omega_G \right) dt'^2 - \frac{dr'^2}{1 + \left( \frac{r'}{2a} \right)^2} - r'^2 \left( 1 - \frac{r'^2}{4a^2} \right) d\phi'^2 - dz'^2 + 2r'^2 \left( \Omega_G - \left( 1 - \frac{r'^2}{4a^2} \right) \Omega_D \right) dt' d\phi' .$$

The conditions (5) for the corresponding metric coefficients in the rotating frame lead to the restrictions

$$c^2 - r'^2 \Omega_D^2 \left( 1 - \frac{r'^2}{4a^2} \right) + 2r'^2 \Omega_D \Omega_G > 0$$

and

$$0 \leq r' < r_G$$

on the radial coordinate  $r'$  and the rotation rate  $\Omega_D$ . Indeed, these conditions lead to a nontrivial region  $G$  of allowed radii  $r'$  with respect to the chosen  $\Omega_D$ .

We again denote the radius of the circular light path by  $r'_0$ . When we insert the relevant coefficients  $g'_{00}$  and  $g'_{02}$  into formula (9) and take into account the rotation scalar (21) we find the Sagnac time delay

$$\Delta\tau'_S = -\frac{4\pi}{c} \frac{r_0'^2 \left( \Omega_G - \left( 1 - \frac{r_0'^2}{4a^2} \right) \Omega_D \right)}{\sqrt{c^2 + r_0'^2 \Omega_D \left( 2\Omega_G - \left( 1 - \frac{r_0'^2}{4a^2} \right) \Omega_D \right)}} .$$

The special choice

$$\Omega_D \equiv \frac{\Omega_G}{1 - \frac{r_0'^2}{4a^2}} . \quad (35)$$

of the rotation rate of the detector leads to a vanishing time delay  $\Delta\tau'_S$  between the two counter-propagating light pulses. Hence, for infinitesimal radii  $r'_0$ , the rotation velocity  $\Omega_D$  of the detector is equal to the rotation scalar  $\Omega_G$  of Gödel's Universe.

### 4.3 A Different Choice of Spatial Coordinates

We now return to the Sagnac time delay measured in the rest-frame of the ideal fluid of Section 4.1. According to equation (34) the Sagnac time delay  $\Delta\tau_S$  depends in a linear way on the rotation scalar  $\Omega_G$  of Gödel's Universe.

We emphasize that this linearity is only due to the special choice of our space coordinates (16) in the line element (17). Indeed, we can also express the Sagnac time delay  $\Delta\tau_S$  in the dimensionless space coordinates of the original Gödel line element (15), where the coordinate transformation (16) does not change the frame of reference. In these coordinates (14) the Sagnac time delay reads

$$\Delta\tau_S = -\frac{8\pi}{\Omega_G} \sinh^2 \bar{r}_0 . \quad (36)$$

Although in this representation the dependence of  $\Delta\tau_S$  on  $\Omega_G$  differs from that of equation (34) both formulae contain the same physics. This invariance is hidden behind the explicit dependence of  $\Delta\tau_S$  in (34) and (36) on the spatial coordinates, which have no immediate physical meaning. In the next section we are going to rectify this problem by introducing an invariant formulation via an operational definition of the radial coordinate.

## 5 Invariant Formulation of the Sagnac Time Delay

The different formulae (34) and (36) for the Sagnac time delay bring out most clearly the question: How can we reformulate the radial coordinate of the mirrors in a measurable quantity?

In the present section we outline a measurement strategy to address this question and then reformulate the Sagnac time delay solely in terms of proper times of light signals. The obtained relation allows for an interesting comparison to expression (13) for the Sagnac time delay in a rotating frame of reference.

### 5.1 Operational Definition of the Radial Coordinate

All expressions for the Sagnac time delay derived so far contain a radial coordinate. What is a measurement strategy for obtaining the radius  $r_0$  of the circular path of the light pulses?

We answer this question in the spirit of [11, 52, 53]. We send light signals along their null geodesics from the center of the circle to every mirror  $M$  in the  $z = 0$  plane, as illustrated on the left side of Figure 3. The mirrors are arranged in such a way as to reflect the light back to the point of emission. Moreover they are lined up in the  $z = 0$  plane as to ensure that the pulses emitted simultaneously at the center and reflected from the mirrors all return to the center at the same time.

Hence, the radius  $r_0$  can be expressed by the proper time  $\Delta\tau_M$  between the emission and detection of the reflected pulses measured by an observer resting at the origin  $r = 0$ . Once the circular setup of mirrors has been established by this operational procedure the mirrors have to be readjusted to guide the counter-propagating light rays in this circular Sagnac configuration with radius  $r_0$ , as indicated in the right of Figure 3.

We conclude by emphasizing that our experimental implementation is only the simplest conceivable model. It is a gedanken experiment, which even requires an infinite amount of mirrors. However, a practical realization has many caveats which need to be considered, such as the finite number of mirrors, the propagation of the light pulses on null geodesics in-between and the applicability of geometrical optics. In fact, the case of a finite number of mirrors has been carried out in principle by [40, 54], where the Sagnac time delay in a rotating frame in Minkowski spacetime serves as an example of the given method.

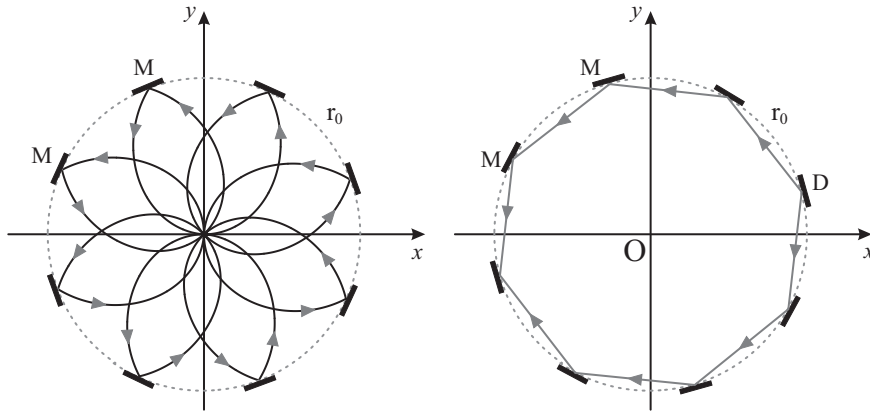


Figure 3: Illustration of the measurement procedure for the radius  $r_0$  of a circle (left) and of the Sagnac time delay  $\Delta\tau_S$  (right). Light rays start at the origin and propagate on null geodesics to the mirrors (M), where they are reflected back to the origin (left). The proper time  $\Delta\tau_M$  between emission and arrival of the light pulses is measured by an observer resting at the origin. The figure on the right illustrates the typical experimental arrangement for the Sagnac effect with a detector (D) on the circle. The straight lines between two consecutive mirrors are an approximation to the corresponding null geodesics. However, the curves shown on the left are exact null geodesics (see Appendix B).

## 5.2 Invariant Formulation

We are now in a position to establish a connection between the Sagnac time delay  $\Delta\tau_S$  and the rotation scalar  $\Omega_G$  in terms of the proper time interval  $\Delta\tau_M$ , measured by an observer resting at the origin  $r = 0$  of the coordinate system. We start by calculating the coordinate time for the light pulses to propagate to the mirrors and back. For this purpose we recall (28) – (30). We then translate this time interval into proper time and express the radius  $r_0$  by the Sagnac time delay making use of equation (34).

Since our mirrors are positioned at the radius  $r_0 < r_G$  the curve parameter  $\lambda_0$  corresponding to this radius can be found from equation (28). Within a period  $0 \leq \eta\lambda < 2\pi$  two values of  $\lambda$  correspond to  $r_0$  and we choose the first solution  $\lambda_0$  within the interval  $0 < \eta\lambda_0 < \pi$ . The coordinate time between the emission of a light pulse at  $r = 0$  and the reflection of it from  $r = r_0$  follows from (30) and (31) and reads

$$t(\lambda_0) = -u^0(0) \lambda_0 + \frac{2}{\Omega_G} \arctan \left( \sqrt{2} \tan(\eta\lambda_0/2) \right). \quad (37)$$

Since Gödel's metric is stationary, spatially homogeneous and possesses rotational symmetry in the planes  $z = \text{const.}$ , it takes twice the time  $t(\lambda_0)$  to travel to and from the mirrors. For an observer resting at the origin  $r = 0$  the proper time  $\Delta\tau_M$  between emission and arrival of the light pulses is given by  $ds = c d\tau = c dt$ , and consequently

$$\Delta\tau_M = 2t(\lambda_0).$$



When we use equation (28) for  $\lambda_0$  in (37) we arrive at the expression

$$\Omega_G \Delta\tau_M = -2\sqrt{2} \arcsin\left(\frac{r_0}{2a}\right) + 4 \arctan\left(\frac{\sqrt{2}\left(\frac{r_0}{2a}\right)}{\sqrt{1 - \left(\frac{r_0}{2a}\right)^2}}\right) \quad (38)$$

for the proper time  $\Delta\tau_M$ . Here we have recalled the definition (29).

In order to make the connection to the absolute value of the Sagnac time delay  $\Delta\tau_S$ , we recall from (34) the relation

$$|\Delta\tau_S| = \frac{4\Omega_G}{c^2} \pi r_0^2 = \frac{8\pi}{\Omega_G} \left(\frac{r_0}{2a}\right)^2,$$

keeping in mind, that the negative value of  $\Delta\tau_S$  is only due to a faster propagation of the light pulse in the positive angular direction.

This formula allows us to express the radius  $r_0$  in (38) in terms of the absolute value  $|\Delta\tau_S|$  of the Sagnac time delay. In order to avoid the appearance of the square root of  $\Delta\tau_S$  it is convenient to introduce the dimensionless parameters

$$\Delta_S^2 \equiv \frac{1}{8\pi} \Omega_G |\Delta\tau_S| = \left(\frac{r_0}{2a}\right)^2 \quad (39)$$

with  $0 < \Delta_S < 1$  and

$$\Delta_M^2 \equiv \frac{1}{8\pi} \Omega_G \Delta\tau_M. \quad (40)$$

When we replace the proper time  $\Delta\tau_M$  and the radius  $r_0$  in (38) by their corresponding dimensionless parameters (39) and (40) we arrive at the transcendental equation

$$4\pi\Delta_M^2 = 2 \arctan\left(\frac{\sqrt{2}\Delta_S}{\sqrt{1 - \Delta_S^2}}\right) - \sqrt{2} \arcsin \Delta_S. \quad (41)$$

This relation is quite a remarkable result since it provides an invariant formulation of the Sagnac time delay in Gödel's Universe. Indeed, for a given value of the  $\Delta_M$ , that is for the radius of the circular path measured in propagation time  $\Delta\tau_M$  of light, the solution of this equation is the scaled Sagnac time delay  $\Delta_S$ . Since we have scaled all proper times in terms of the rotation scalar the transcendental equation contains no parameters of Gödel's Universe. The information about the metric reflects itself solely in the form of the equation.

### 5.3 Comparison to the Rotating Frame in Flat Spacetime

We now compare the transcendental equation (41) for the Sagnac time delay of Gödel's metric with the corresponding formula for the time delay (13) found in a rotating frame of reference in Minkowski spacetime.

The first step consists of replacing the radial coordinate in equation (13) by a measurable time. For this purpose we apply the same measurement strategy to the rotating frame as

discussed in 5.1. We then substitute the radial coordinate  $r'_0$  by the proper time interval  $\Delta\tau'_M$  of a light ray, which returns after reflection from the circular mirror arrangement at  $r'_0$  to the origin. Since the observer at the origin is at rest relative to the inertial frame of Minkowski spacetime, we find immediately the proper time

$$\Delta\tau'_M = \frac{2r'_0}{c}.$$

For the comparison of the Sagnac time delay (13) with the expression (41) it is useful to introduce the dimensionless parameters

$$\Delta_R'^2 \equiv \frac{1}{8\pi}\Omega_R\Delta\tau'_R \quad (42)$$

and

$$\Delta_M'^2 \equiv \frac{1}{8\pi}\Omega_R\Delta\tau'_M, \quad (43)$$

in complete analogy to the formulae (39) and (40).

Using these parameters we can cast the Sagnac time delay (13) into the form

$$2\Delta_R'^2 = \frac{(4\pi\Delta_M'^2)^2}{\sqrt{1 - (4\pi\Delta_M'^2)^2}},$$

which in contrast to (41) is an explicit formula for  $\Delta_R'$  in terms of  $\Delta_M'$ .

In order to obtain a formula analogous to (41) we solve this equation for  $4\pi\Delta_M'^2$ , which yields

$$4\pi\Delta_M'^2 = \sqrt{2}\Delta_R' \sqrt{\sqrt{1 + \Delta_R'^4} - \Delta_R'^2}. \quad (44)$$

Due to our restriction (12) to the spacetime region  $G'$  the parameter  $\Delta_M'$  has to satisfy the condition

$$0 \leq 4\pi\Delta_M'^2 < 1.$$

Figure 4 illustrates the differences in the curves defined by (41) and (44). We find that for our measurement strategy the difference between the solid and dotted curve is very small. This is surprising, as the underlying physical systems with Gödel's Universe on the one hand and the rotating frame in flat Minkowski spacetime on the other hand, differ substantially in their global behavior.

This similarity can also be understood from the Taylor series expansion of (41) and (44). Indeed, for small values of  $\Delta_S$  or  $\Delta_R'$  we find

$$4\pi\Delta_M'^2 = \sqrt{2} \left( \Delta_S - \frac{1}{2}\Delta_S^3 + \frac{11}{40}\Delta_S^5 + \mathcal{O}(\Delta_S^7) \right), \quad (45)$$

and

$$4\pi\Delta_M'^2 = \sqrt{2} \left( \Delta_R' - \frac{1}{2}\Delta_R'^3 + \frac{1}{8}\Delta_R'^5 + \mathcal{O}(\Delta_R'^7) \right). \quad (46)$$

Thus the two equations determining the Sagnac time delay only differ in the contribution of the fifth power of  $\Delta_S$  or  $\Delta_R'$ .

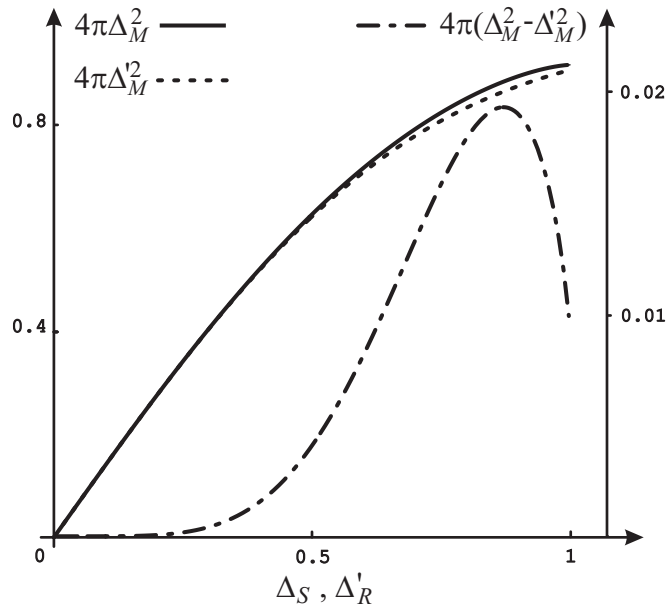


Figure 4: Comparison between the Sagnac time delay for Gödel’s Universe (solid line) and for a rotating coordinate system in flat spacetime (dotted curve). Scaled proper times  $4\pi\Delta_M^2$  and  $4\pi\Delta_M'^2$  of a light signal propagating from the origin to a mirror on the circle and back in Gödel’s Universe and in a rotating frame of reference in flat spacetime, plotted versus the Sagnac time delays  $\Delta_S$  and  $\Delta'_R$  in scaled units. While the left ordinate applies to the absolute values of those scaled time delays, the dashed-dotted line magnifies the residual differences  $4\pi(\Delta_M'^2 - \Delta_M^2)$  as indicated by the right ordinate.

## 6 Summary and Outlook

In conclusion we have investigated the Sagnac time delay in Gödel’s Universe. Our analysis generalizes the results of our previous examination [29], which were limited to small radial dimensions and rotation rates, to arbitrary sizes of the circular Sagnac interferometer and arbitrary rotation rates of Gödel’s Universe. The previous results exhibited a close relation between the Sagnac effect in Gödel’s Universe and in a rotating frame in flat spacetime. By obtaining exact and invariant expressions for the Sagnac time delays in both systems, valid for arbitrary rotation rates and radii within  $G$  and  $G'$ , we have demonstrated inhere, that this statement is also valid in general.

The original Gödel solution is not in agreement with cosmological observations of the background radiation [55]. Therefore, one might be tempted to dismiss this remarkable exact solution of Einstein’s field equations altogether. However, recently analogies between light propagation in curved spacetimes and optics in moving media [31] or sonic propagation in condensed matter systems [32, 33] have instigated renewed interest in this subject. For example, these articles consider experimental analogues of a gravitational black hole. Here, the event horizon emerges when the flow velocities of the optical medium or the condensate exceed the velocities of light or sound in these media, respectively.

How far can we push these analogies? Can we find an optical or sonic realization of the light propagation in Gödel's Universe? Unfortunately, a global simulation of the Gödel spacetime via an experimental analogue seems not to be very probable due to the causal structure of this metric discussed in Section 3.4. But since we can approximate the local light propagation in Gödel's Universe by a rotating coordinate frame in Minkowski spacetime it should be possible to translate the physics of wave propagation in curved space locally to cold quantum gases. Vortices [56, 57, 58] or alternatively Abrikosov lattices [59] might offer a possible route to an analogue of Gödel's Universe in the laboratory.

## 7 Acknowledgments

We thank I. Ciufolini, J. Ehlers, G. Schäfer and G. Süssmann and A. Wolf for many fruitful discussions. Moreover, we have thoroughly enjoyed the stimulating atmosphere at the Hyper meeting in Paris and appreciated the financial support, which made our participation possible. We are also very grateful to C. Lämmerzahl for his editorial efforts.

## A Definitions and Conventions

Throughout this article we use the signature  $(+, -, -, -)$  of our metric  $g_{\mu\nu}$  with the determinant  $g \equiv \det g_{\mu\nu}$  and denote the covariant derivative with a semicolon and the ordinary partial derivative with a comma.

The antisymmetric tensor

$$\varepsilon^{\alpha\beta\gamma\delta} \equiv \frac{1}{\sqrt{-g}} \Delta^{\alpha\beta\gamma\delta}$$

is defined in terms of the Levi-Cevita-Symbol

$$\Delta^{\alpha\beta\gamma\delta} \equiv \left\{ \begin{array}{ll} 1 & \text{for an even permutation} \\ -1 & \text{for an odd permutation} \\ 0 & \text{otherwise} \end{array} \right\}. \quad (47)$$

The components of the Riemann tensor

$$R^\mu_{\alpha\beta\gamma} \equiv \Gamma^\mu_{\alpha\gamma,\beta} - \Gamma^\mu_{\alpha\beta,\gamma} + \Gamma^\mu_{\rho\beta} \Gamma^\rho_{\alpha\gamma} - \Gamma^\mu_{\rho\gamma} \Gamma^\rho_{\alpha\beta}$$

result from the Christoffel symbols

$$\Gamma^\mu_{\alpha\beta} \equiv \frac{1}{2} g^{\mu\nu} (g_{\nu\alpha,\beta} + g_{\nu\beta,\alpha} - g_{\alpha\beta,\nu}).$$

The Ricci tensor and the scalar curvature

$$R_{\alpha\beta} \equiv R^\mu_{\alpha\mu\beta}, \quad R \equiv R^\mu_{\mu}$$

follow by contraction.

The covariant derivative of a contravariant vector field  $T^\alpha$  reads

$$T^\alpha{}_{;\beta} \equiv T^\alpha{}_{,\beta} + \Gamma^\alpha{}_{\mu\beta} T^\mu$$

whereas for a covariant vector field it takes the form

$$T_{\alpha;\beta} \equiv T_{\alpha,\beta} - \Gamma^\mu{}_{\alpha\beta} T_\mu.$$

## B Integration of Null Geodesics

In this Appendix we outline a procedure to obtain the solutions of the geodesic equations in Gödel's metric. Since the main goal of the paper is the Sagnac time delay and in particular, an invariant formulation of it, we confine ourselves to special initial conditions appropriate for our experimental setup.

### B.1 General Idea

The central idea for solving the geodesic equations relies on finding simple expressions for the constants of motion. Some of these constants can easily be obtained if the metric possesses Killing vectors  $\xi^\mu$ . This feature can be understood by contracting the geodesic equations (27) with the contravariant components of a Killing vector, that is

$$\xi_\mu u^\mu{}_{;\nu} u^\nu = (\xi_\mu u^\mu)_{;\nu} u^\nu - \xi_{\mu;\nu} u^\mu u^\nu = 0.$$

When we recall the Killing equation (24) and note, that the covariant derivative of a scalar is just the ordinary partial derivative, we find

$$\frac{d}{d\lambda} (\xi_\mu u^\mu) = 0.$$

Hence, every Killing vector corresponds to a constant of motion.

In addition the norm of the tangent vector  $u^\mu(\lambda)$  is constant along the geodesics and therefore yields another constant of motion

$$g_{\mu\nu} u^\mu u^\nu = \epsilon^2. \tag{48}$$

Since the metric coefficients (18) depend only on the radial coordinate  $r$ , the solution of the geodesic equations (27) can be found by making use of the first three Killing vectors in (25) to obtain the simple constants of motion

$$A = u_0(\lambda) = c^2 u^0(\lambda_0) + r^2(\lambda_0) \Omega_G u^2(\lambda_0) \tag{49}$$

$$B = u_2(\lambda) = r^2(\lambda_0) \Omega_G u^0(\lambda_0) - r^2(\lambda_0) \left( 1 - \left( \frac{r(\lambda_0)}{2a} \right)^2 \right) u^2(\lambda_0) \tag{50}$$

$$C = u_3(\lambda) = -u^3(\lambda_0). \tag{51}$$

Here  $\lambda_0$  denotes the initial curve parameter and in the second step of these equations we have made use of the relation  $u_\mu(\lambda_0) = g_{\mu\nu}(\lambda_0)u^\nu(\lambda_0)$  with the metric coefficients (18).

We substitute the expressions (49)–(51) for the covariant components of the four-velocity  $u^\mu$  into the constant of motion (48) and find with the contravariant metric coefficients

$$(g^{\mu\nu}) = \begin{pmatrix} \frac{1}{c^2} \frac{1 - \left(\frac{r}{2a}\right)^2}{1 + \left(\frac{r}{2a}\right)^2} & 0 & \frac{\Omega_G}{c^2} \frac{1}{1 + \left(\frac{r}{2a}\right)^2} & 0 \\ 0 & -\left(1 + \left(\frac{r}{2a}\right)^2\right) & 0 & 0 \\ \frac{\Omega_G}{c^2} \frac{1}{1 + \left(\frac{r}{2a}\right)^2} & 0 & -\frac{1}{r^2} \frac{1}{1 + \left(\frac{r}{2a}\right)^2} & 0 \\ 0 & 0 & 0 & -1 \end{pmatrix}. \quad (52)$$

the equation

$$g^{\mu\nu}u_\mu u_\nu = \frac{A^2}{c^2} \frac{1 - \left(\frac{r}{2a}\right)^2}{1 + \left(\frac{r}{2a}\right)^2} + \frac{\Omega_G}{c^2} \frac{2AB}{1 + \left(\frac{r}{2a}\right)^2} - \frac{B^2}{r^2} \frac{1}{1 + \left(\frac{r}{2a}\right)^2} - C^2 - \left(1 + \left(\frac{r}{2a}\right)^2\right) (u_1(\lambda))^2 = \epsilon^2. \quad (53)$$

Inserting  $u_1 = g_{11}u^1$  into this expression yields a differential equation in the radial coordinate  $r$ . The solution  $r(\lambda)$  can then be used to formulate the differential equations for the coordinates  $t$  and  $\phi$  by making use of the relations  $u^0 = g^{0\mu}u_\mu$  and  $u^2 = g^{2\mu}u_\mu$ . The solution of the third spatial coordinate  $z$  can be obtained from the last constant of motion (51)

$$u^3 = g^{33}u_3 = -C, \quad z(\lambda) = u^3(\lambda_0)(\lambda - \lambda_0) + z(\lambda_0). \quad (54)$$

Thus, the motion in  $z$ -direction is like a free motion in one dimension in flat Minkowski spacetime.

## B.2 Special Initial Condition

In the remainder of this Appendix we focus on the solution of the geodesic equations for light, that is  $\epsilon = 0$  in (48), subjected to the special initial conditions associated with the experimental arrangement considered in Section 5. In particular, the light pulse starts with the initial curve parameter  $\lambda_0 = 0$  at the position  $r(0) = 0$ ,  $z(0) = 0$  and propagates in the  $z = 0$  plane. Therefore, we have to choose  $u^3(0) = 0$ . We emphasize, that for  $r = 0$  the angle velocity  $u^2(0)$  loses its meaning. Moreover, since we start at the origin and  $r$  is positive, we have to take  $u^1(0) > 0$ .

These special initial conditions reduce the constants of motion (49)–(51) to

$$A = u_0(\lambda) = c^2 u^0(0) > 0 \quad (55)$$

$$B = u_2(\lambda) = 0 \quad (56)$$

$$C = u_3(\lambda) = 0. \quad (57)$$

These compact expressions allow us to integrate the differential equation (53) for our radial coordinate  $r(\lambda)$  as shown in the next section.

### B.3 Radial Coordinate

The constants of motion (55)–(57) reduce the differential equation (53) to

$$c^2 \left( 1 - \left( \frac{r}{2a} \right)^2 \right) (u^0(0))^2 - \left( 1 + \left( \frac{r}{2a} \right)^2 \right)^2 (u_1(\lambda))^2 = 0,$$

which leads with  $u_1 = g_{11} u^1$  and  $u^1(0) > 0$  to

$$\frac{dr}{d\lambda} = \pm c u^0(0) \sqrt{1 - \left( \frac{r}{2a} \right)^2}. \quad (58)$$

The two equations correspond to the two different signs of the radial velocity.

Separation of variables

$$\int_0^{r(\lambda)} \frac{dr}{\sqrt{1 - \left( \frac{r}{2a} \right)^2}} = \pm c u^0(0) \int_0^\lambda d\lambda$$

finally yields the radial geodesic

$$\frac{r(\lambda)}{2a} = \left| \sin \left( \frac{1}{2} \eta \lambda \right) \right|. \quad (59)$$

Here we have introduced the periodicity rate

$$\eta \equiv \sqrt{2} u^0(0) \Omega_G \quad (60)$$

in such a way, that one cycle of the radial coordinate  $r(\lambda)$  corresponds to the curve parameter  $\lambda = 2\pi/\eta$ .

It is apparent, that the solution (59) is not differentiable at  $r = 0$ . This feature is due to the transformation to polar coordinates, which is singular at  $r = 0$ . Furthermore we recognize that these null geodesics touch the critical Gödel radius  $r_G = 2a$  for  $\eta\lambda = \pi$ .

### B.4 Coordinate Time

The explicit expression (59) for our radial coordinate allows us now to find the corresponding expressions for both the coordinate time  $t(\lambda)$  and the angular coordinate  $\phi(\lambda)$ . For this purpose we use the relation  $u^0 = g^{0\mu} u_\mu$  with the contravariant metric coefficients (52) and the constants of motion (55) and (56) and arrive at

$$u^0(\lambda) = u^0(0) \frac{1 - \left( \frac{r(\lambda)}{2a} \right)^2}{1 + \left( \frac{r(\lambda)}{2a} \right)^2} \geq 0.$$

Hence, the coordinate time is increasing monotonously.

Substitution of (59) into the above equation leads to

$$t(\lambda) = -u^0(0) \lambda + 2u^0(0) \int_0^\lambda \frac{d\lambda}{1 + \sin^2\left(\frac{1}{2}\eta\lambda\right)}, \quad (61)$$

which after integration yields

$$t(\lambda) = -u^0(0) \lambda + \frac{2}{\Omega_G} \left( \arctan\left(\sqrt{2} \tan(\eta\lambda/2)\right) + m(\lambda) \pi \right). \quad (62)$$

Here we have used (60) and introduced the integer

$$m(\lambda) \equiv \left[ \frac{\eta\lambda}{2\pi} + \frac{1}{2} \right]_I \quad (63)$$

where the brackets denote the greatest integer less than or equal to the number inside them. The integer  $m$  guarantees the continuity, differentiability and monotony of  $t(\lambda)$  for arbitrary  $\lambda \geq 0$ .

## B.5 Angular Coordinate

The dependence of the angular coordinate  $\phi(\lambda)$  on the curve parameter can be found in a way similar to the one of the coordinate time  $t(\lambda)$ . With the help of the relation  $u^2 = g^{2\mu}u_\mu$  and the constants of motion (55) and (56) we arrive at

$$u^2(\lambda) = \frac{u^0(0) \Omega_G}{1 + \left(\frac{r(\lambda)}{2a}\right)^2}.$$

Since the angular velocity  $u^2$  loses its meaning at the point  $r = 0$  we perform the integration over one cycle only, that is  $0 \leq \lambda < (2\pi)/\eta$ . In this case the integral

$$\phi(\lambda) = \phi(0) + u^0(0) \Omega_G \int_0^\lambda \frac{d\lambda}{1 + \sin^2\left(\frac{1}{2}\eta\lambda\right)}$$

leads in analogy to (61) under the restriction  $m(\lambda) = 0, 1$  to the angular coordinate

$$\phi(\lambda) = \phi(0) + \arctan\left(\sqrt{2} \tan(\eta\lambda/2)\right) + m(\lambda) \pi.$$

We can rewrite this expression in order to allow arbitrary values of  $\lambda > 0$  which results in

$$\phi(\lambda) = \phi(0) + \arctan\left(\sqrt{2} \tan(\eta\lambda/2)\right) + \left(m(\lambda) - m\left(\lambda - \frac{\pi}{\eta}\right)\right) \pi. \quad (64)$$

Equations (59), (62) and (64) represent the null geodesics for our special initial conditions.



## References

- [1] Aczel, A. (2003). "Pendulum: Leon Foucault and the Triumph of Science", New York: Pocket Books
- [2] Sagnac, G. (1913). C. R. Acad. Sci., Paris **157**, 708
- [3] Sagnac, G. (1913). C. R. Acad. Sci., Paris **157**, 1410
- [4] Post, E. J. (1967). Rev. Mod. Phys. **39**, 475
- [5] Tartaglia, A. (1998). Phys. Rev. D **58**, 064009
- [6] Nandi, K. K., Alsing, P. M., Evans, J. C., Nayak, T. B. (2001). Phys. Rev. D **63**, 084027
- [7] Michelson, A. A., Gale, H. G. (1925). Astrophys. J. **61**, 140
- [8] Weyl, H. (1924). Naturwissenschaften **12** 197
- [9] Isenberg, J., Wheeler, J. A. (1979) Relativity, Quanta and Cosmology (New York: Johnson Reprint Corporation)
- [10] Ciufolini, I, Wheeler, J. A. (1995). Gravitation and Inertia (Princeton, NJ: Princeton University Press)
- [11] Ohanian, H. C. (1976) Gravitation and Spacetime (Norton and Company, New York, 1976)
- [12] Schleich, W. P., Scully. M. O. (1984). New Trends in Atomic Physics (Les Houches 1982, Session XXXVI) eds. G. Grynberg and R. Stora (Amsterdam: North-Holland)
- [13] Bonnor, W. B., Steadman, B. R. (1999). Class. Quantum Grav. **16**, 1853
- [14] Lämmerzahl, C., Everitt, C. W. F., Hehl, F. W. (2000). Gyros, Clocks, Interferometers: Testing Relativistic Gravity in Space (Heidelberg Springer)
- [15] Ciufolini, I., Pavlis, E., Chieppa, F., Fernandes-Vieira, E. Pérez-Mercader, J. (1998). Science **279**, 2100
- [16] Thirring, H. (1918). Phys. Z. **19**, 33
- [17] Thirring, H. (1921). Phys. Z. **22**, 29
- [18] Lense, J., Thirring, H. (1918). Phys. Z. **19**, 156
- [19] Mashoon, B., Hehl, F. W., Theiss, D. S. (1984). Gen. Rel. Grav. **16**, 711
- [20] HYPER 2000 Hyper-precision cold atom interferometry in space, Assessment Study Report, European Space Agency
- [21] Gustavson, T. L., Bouyer, P., Kasevich, M. A. (1997). Phys. Rev. Lett. **78**, 2046
- [22] Gustavson, T. L., Landragin, A., Kasevich, M. A. (2000). Class. Quantum Grav. **17**, 2385
- [23] Bordé, Ch. J. (2001). C. R. Acad. Sci. Paris, t.2, Série IV, 509
- [24] Bordé, Ch. J., Karasiewicz, A., Tournenc, Ph. (1994). Int. J. Mod. Phys. D **3**, 157
- [25] Gödel, K. (1949). Rev. Mod. Phys. **21**, 447

- [26] Gödel, K., (1949). Albert Einstein: Philosopher-Scientist, ed. P. A. Schilpp, The Library of Living Philosophers Vol. VII (Evanston, Illinois), p. 557
- [27] Gödel, K. (1950). Proc. Int. Cong. Math. vol. 1, p. 175
- [28] Hawking, S. W., Ellis, G. F. R. (1973). The large scale structure of space-time, Cambridge University Press
- [29] Delgado, A., Schleich, W. P., Süßmann, G. (2002). NJP **4**, 37.1
- [30] see e.g.: [www.esf.org/publication/120/COSLAB.pdf](http://www.esf.org/publication/120/COSLAB.pdf)
- [31] Leonhardt, U., Piwnicki, P. (1999). Phys. Rev. A **60**, 4301
- [32] Volovik, G. E. (2003). The Universe in a Helium Droplet, Oxford Univ. Pr.
- [33] Garay, L. J., Anglin, J. R., Cirac, J. I., Zoller, P. (2001). Phys. Rev. A **63**, 023611
- [34] Cohen, J. M., Vishveshwara, C. V., Dhurandhar, S. V. (1980). J. Phys. A **13**, 933
- [35] Kajari, E. (2003), Untersuchungen zum Gödeluniversum, Diploma Thesis, University of Ulm
- [36] Chow, W. W., Gea-Banacloche, J., Pedrotti, L. M., Sanders, V. E., Schleich, W. P., Scully, M. O. (1985). Rev. Mod. Phys. **57**, 61
- [37] Scully, M. O., Zubairy, M. S., Haugan, M. P. (1981). Phys. Rev. A **24**, 2009
- [38] Hannay, J. H. (1985). J. Phys. A **18**, 221
- [39] Cohen, J. M., Moses, H. E., Rosenblum, A. (1983). Phys. Rev. Lett. **51**, 1501
- [40] Bazański, S. L. (1998). Particles, Fields, and Gravitation, ed. J. Rembieliński, AIP Conf. Proc. **453**, 421 (see p. 428)
- [41] Landau, L. D., Lifschitz, E. M. (1992). Lehrbuch der theoretischen Physik, Bd. 2: Klassische Feldtheorie, 12. Auflage, Akademie Verlag, Berlin, p.303
- [42] Ehlers J. (1961). Beiträge zur relativistischen Mechanik kontinuierlicher Medien, Abh. Mainzer Akad. Wiss. Math.-Nat. Klasse 1961 Nr. 11
- [43] See e.g. Novello, M., Svaiter, N. F., Guimarães, M. E. X. (1993). Gen. Rel. Grav. **25**, 137
- [44] Kerr, R. P. (1963). Phys. Rev. Lett. **11**, 237
- [45] Carter, B. (1968). Phys. Rev. **174**, 1559
- [46] Stockum, W. J. (1937). Proc. Roy. Soc. Edinburgh **57**, 135
- [47] Mallett, R. L. (2003). Found. Phys. **33**, 1307
- [48] Kundt, W. (1956). Zeitschrift für Physik **145**, 611
- [49] Chandrasekhar, S., Wright, J. P. (1961). Proc. Nat. Acad. Sci. **47**, 341
- [50] Novello, M., Damiano Soares, I., Tiomno, J. (1983). Phys. Rev. D **27**, 779
- [51] Ciufolini, I., Kopeikin, S. Mashoon, B. Ricci, F. (2002). arXiv: gr-qc/0210015
- [52] Marzke, R. F., Wheeler, J. A. (1964) in: Gravitation and Relativity, ed. Chiu H.-Y. and Hoffman W. F. (Benjamin, New York, 1964)

- [53] Bodenner, J., Will, C. M. (2003). *Am. J. Phys.* **71**, 770
- [54] Bazański, S. L. (1999). *On Einstein's Path*, ed. A. Harvey, Springer, New York
- [55] Bunn, E. F., Ferreira, P. G., Silk, J. (1996). *Phys. Rev. Lett.* **77**, 2883
- [56] Williams, J. E., Holland, M. (1999). *Nature* **401**, 568
- [57] Fetter, A. (2002). *JLTP* **129**, 263
- [58] Nandi, G., Walser, R., Schleich W. P. (2004). *Phys. Rev. A* **69**, 063606
- [59] Anglin, J. R., Ketterle, W. (2002). *Nature* **416**, 211